Chemical Geology xxx (2011) xxx–xxx

Contents lists available at ScienceDirect

Chemical Geology

journal homepage: www.elsevier.com/locate/chemgeo

Research paper

Volatile abundances and oxygen isotopes in basaltic to dacitic lavas on mid-ocean ridges: The role of assimilation at spreading centers

V.D. Wanless [a,*], M.R. Perfit [a], W.I. Ridley [b,c], P.J. Wallace [d], C.B. Grimes [e,1], E.M. Klein [f]

[a] Department of Geological Sciences, University of Florida, Gainesville, FL 32611, United States
[b] US Geological Survey, Denver, CO 80225, United States
[c] National Science Foundation, Arlington, VA 22230, United States
[d] Department of Geological Sciences, University of Oregon, Eugene, OR 97403, United States
[e] Department of Geosciences, Mississippi State, MS 39762, United States
[f] Nicholas School of the Environment, Duke University, Durham, NC 27708, United States

ARTICLE INFO

Article history:
Received 2 November 2010
Received in revised form 25 May 2011
Accepted 26 May 2011
Available online xxxx

Editor: L. Reisberg

Keywords:
Assimilation
Chlorine
Dacite
Mid-ocean ridge
Oxygen isotopes
Volatiles

ABSTRACT

Most geochemical variability in MOR basalts is consistent with low- to moderate-pressure fractional crystallization of various mantle-derived parental melts. However, our geochemical data from MOR high-silica glasses, including new volatile and oxygen isotope data, suggest that assimilation of altered crustal material plays a significant role in the petrogenesis of dacites and may be important in the formation of basaltic lavas at MOR in general. MOR high-silica andesites and dacites from diverse areas show remarkably similar major element trends, incompatible trace element enrichments, and isotopic signatures suggesting similar processes control their chemistry. In particular, very high Cl and elevated H_2O concentrations and relatively light oxygen isotope ratios (~5.8‰ vs. expected values of ~6.8‰) in fresh dacite glasses can be explained by contamination of magmas from a component of ocean crust altered by hydrothermal fluids. Crystallization of silicate phases and Fe-oxides causes an increase in $\delta^{18}O$ in residual magma, but assimilation of material initially altered at high temperatures results in lower $\delta^{18}O$ values. The observed geochemical signatures can be explained by extreme fractional crystallization of a MOR basalt parent combined with partial melting and assimilation (AFC) of amphibole-bearing altered oceanic crust. The MOR dacitic lavas do not appear to be simply the extrusive equivalent of oceanic plagiogranites. The combination of partial melting and assimilation produces a distinct geochemical signature that includes higher incompatible trace element abundances and distinct trace element ratios relative to those observed in plagiogranites.

1. Introduction

Crustal assimilation has been proposed in the petrogenesis of some mid-ocean ridge (MOR) magmas (e.g., O'Hara, 1977; Michael and Schilling, 1989; Michael and Cornell, 1998), but for several reasons it is largely ignored as a primary igneous process in ridge settings. First, contamination is commonly overlooked because most geochemical variations in MOR lavas can be readily explained by fractional crystallization, variations in mantle melting parameters, or differences in mantle source compositions. Second, the low volumes of melt assimilated compared to the more voluminous mid-ocean ridge basalt (MORB) magma makes assimilation difficult to identify in the erupted lavas. Third, the magma and wall rock may have similar major and trace element compositions, resulting in melts that are geochemically difficult to discriminate from typical MORB lavas. However, variable degrees of hydrothermal alteration of basaltic crust can produce significant changes in fluid mobile elements and ratios of low-mass isotopes in oceanic rocks depending on the water/rock ratios (e.g., Alt and Teagle, 2000). Therefore, components that are particularly sensitive to seawater interaction, such as Cl, U, H_2O, and oxygen isotopes, can be used to determine the extent to which crustal assimilation is involved in MOR magmatism.

Contamination of MOR magmas by seawater-altered rocks was first proposed based on excess Cl in MORB glasses (Michael and Schilling, 1989; Michael and Cornell, 1998). The elevated Cl concentrations compared to elements of similar incompatibility (K, Nb, Ti) in fresh MORB glass cannot be explained by post-eruption alteration or fractional crystallization and are instead attributed to assimilation of a seawater-derived component such as saline brines or altered ocean crust (Michael and Schilling, 1989; Michael and Cornell, 1998). Subsequently, Cl over-enrichment has been identified in many submarine settings, including MOR (Perfit et al., 1999; Coogan et al., 2003; le Roux et al., 2006; Wanless et al., 2010), back-arc basins (Kent et al., 2002; Sun et al., 2007) and ocean islands (e.g. Kent et al., 1999).

* Corresponding author at: Department of Geology and Geophysics, MS#24, WHOI, Woods Hole, MA 02541, United States. Tel.: +1 508 289 3922.
E-mail address: dwanless@whoi.edu (V.D. Wanless).
[1] Previous address: Department of Geological Science, University of Wisconsin, Madison, WI 53706, United States.

0009-2541/$ – see front matter © 2011 Elsevier B.V. All rights reserved.
doi:10.1016/j.chemgeo.2011.05.017

Despite the clear evidence of assimilation in these lavas, many models for the magmatic plumbing system at MORs continue to ignore this process.

An alternate approach to identifying crustal contamination on MORs is through oxygen isotope ratios. Low oxygen isotope ratios relative to mantle values are observed in many lavas from Icelandic volcanoes (e.g. Gautason and Muehlenbach, 1998). Lower-than-mantle values have also been observed in olivine phenocrysts and in Hawaiian glasses and are attributed to assimilation of altered Pacific crust (Eiler et al., 1996; Garcia et al., 1998). Decreases in $\delta^{18}O$ relative to primary mantle-like values are attributed to contamination by crustal rocks altered at temperatures >200–250 °C, which have lower values due to the temperature-dependent fractionation of oxygen isotopes between seawater and mineral phases in ocean crust during high-temperature hydrothermal alteration (Muehlenbach and Clayton, 1972; Alt et al., 1996). Subsequent assimilation of altered crust in contact with MOR melt should lower the oxygen isotope ratios of the resulting magma. If the mass of assimilant relative to the parent magma is low it may be difficult to detect a decrease in the oxygen isotope ratios. However, oxygen isotopes may be substantially modified in magmas that have experienced more significant degrees of assimilation.

Here, we examine H_2O, CO_2 and S concentrations and oxygen isotope ratios from a suite of lavas collected at the 9°N overlapping spreading center (OSC) on the East Pacific Rise (EPR) to further evaluate their petrogenesis, with specific emphasis on the role of crustal assimilation, and to test the more general hypothesis that assimilation is a common process in MOR magmatic systems. This suite of lavas displays a nearly continuous range of compositions from basalts to dacites, including one of the most evolved lava compositions sampled on a MOR (67.46 wt.% SiO_2). Major and trace element data and Cl concentrations indicate that assimilation of altered ocean crust is a critical process for the formation of MOR dacites (Wanless et al., 2010); a process that should also be reflected in the H_2O and CO_2 concentrations and oxygen isotope ratios. H_2O, CO_2 and S concentrations are used to provide information on degassing of high-silica magmas during extensive fractional crystallization and eruption on the seafloor. We use Cl/K_2O and Ce/H_2O ratios to constrain the composition of the assimilant, which may be altered ocean crust, saline brines and/or seawater.

2. Background

2.1. Geologic setting

The 9°N OSC (Fig. 1) is located between the Clipperton and Siquieros transform faults on the EPR. It is a second order ridge discontinuity consisting of limbs that overlap by ~27 km and offset the ridge axis ~8 km from east to west (Sempere and Macdonald, 1986). The OSC has been migrating southward at a rate of approximately 42 km/Myr such that the eastern limb propagates into older crust and the western limb recedes or dies (Macdonald and Fox, 1983; Carbotte and Macdonald, 1992).

The 9°N OSC is one of the most extensively studied OSCs on the MOR system. It has been the focus of several geophysical studies (Detrick et al., 1987; Harding et al., 1993; Kent et al., 1993, 2000; Bazin et al., 2001; Dunn et al., 2001; Tong et al., 2002), which have produced the first 3D multi-channel seismic survey of a mid-ocean ridge (Kent et al., 2000) and a 3D seismic refraction study (Dunn et al., 2001). These studies reveal shallow melt lenses beneath both limbs of the OSC and in the interlimb region north of the overlap basin (Kent et al., 2000). The western, receding limb melt lens is narrow and shows no significant variation in depth along axis (Kent et al., 2000), while the melt lens beneath the eastern, propagating limb shows variations in both width and depth. Beneath the southern portion of the east limb the melt lens is narrower and deeper than the rest of the eastern ridge axis, plunging ~500 m southward over ~6 km (Kent et al., 2000). North of the overlap basin, the melt lens is anomalously wide (>4 km) and is not centered directly over the ridge axis, instead extending from the axis ~4 km to the west (Kent et al., 2000; Tong et al., 2002). Although the depth of the lens varies along axis, according to interpretation of seismic data, the top of the melt lens appears to track the base of the sheeted dikes, at approximately 1.5–2 km beneath the seafloor (Kent et al., 2000; Tong et al., 2002).

The first lava sampling in this region occurred during the CHEPR dredging and wax coring cruise that recovered several high-silica lavas, along with basalts and FeTi basalts (Langmuir et al., 1986). More recently, the 9°N OSC was the focus of the *MEDUSA2007* research cruise (AT15-17), which completed detailed mapping using the DSL-120A side-scan system (White et al., 2009), and the WHOI TowCam (Fornari, 2003) and extensive sampling using the ROV *Jason2*, (Wanless et al., 2010). Results of this cruise revealed that the region has erupted a range of rock types from basalts to dacites, but that high-silica lavas are confined to the eastern propagating limb of the OSC (Wanless et al., 2010). More evolved compositions on MOR are often associated with ridge propagation, where magmas are in contact with older volcanic crust (e.g., Christie and Sinton, 1981). The andesites and dacites were primarily collected north of 9°06′ N either on-axis or on the flanks of the axial graben (Fig. 1). They erupted above the eastern edge of the seismically imaged wide melt lens. Several andesites/dacites were collected along a linear pillow mound that hosted the only active hydrothermal venting observed at the OSC. Lavas erupted at the OSC are dominantly ferrobasalts in contrast to the more MgO-rich MORB lavas that dominate the 9°15′ N to 10°N section of the EPR (Batiza and Niu, 1992; Perfit et al., 1994; Smith et al., 2001; Goss et al., 2010).

2.2. Evidence of assimilation on MOR

Fractional crystallization is likely the primary process involved in basalt differentiation on MORs, however, there is geochemical, observational, and experimental evidence of assimilation occurring in these settings. As noted above, elevated Cl concentrations in some MORB cannot be a consequence of fractional crystallization alone and are instead explained by assimilation (Michael and Schilling, 1989; le Roux et al., 2006). Experimental studies suggest that low-degree partial melting of the upper ocean crust is possible and may account for the ubiquitous presence of plagiogranite veins throughout the ocean crust (Koepke et al., 2007). This is supported by observations of the transition zone between the gabbro (frozen melt lens) and sheeted dike complex in ophiolites, which show evidence of partial melting of wall rock (e.g. Coogan, 2003).

Assimilation is also an important process in the petrogenesis of dacites on MOR. Previous geochemical studies of dacites erupted at the 9°N OSC have used major and trace element concentrations in conjunction with petrologic modeling to show that extensive fractional crystallization (up to 95%) alone cannot explain the major and trace element concentrations of the dacitic lavas (Wanless et al., 2010). Instead, compositions of high-silica lavas (including elevated chlorine concentrations) suggest that incorporation of a seawater-altered component (i.e., altered oceanic crust, seawater, and/or brines) is important in their petrogenesis. Thus it can be concluded that the petrogenesis of MOR dacites requires melting and assimilation of altered crustal material into a fractionally crystallizing magma chamber (i.e., an assimilation and fractional crystallization process; AFC).

2.3. Composition of potential assimilants

Possible sources of assimilants include seawater modified by hydrothermal circulation, saline brines stored within the crust, and/or altered crustal material (gabbros or sheeted dikes). Saline brines form from high temperature phase separation of seawater during hydrothermal circulation (e.g., Berndt and Seyfreid, 1990) and may be trapped along grain boundaries or in pore spaces within the ocean

Please cite this article as: Wanless, V.D., et al., Volatile abundances and oxygen isotopes in basaltic to dacitic lavas on mid-ocean ridges: The role of assimilation at spreading centers, Chem. Geol. (2011), doi:10.1016/j.chemgeo.2011.05.017

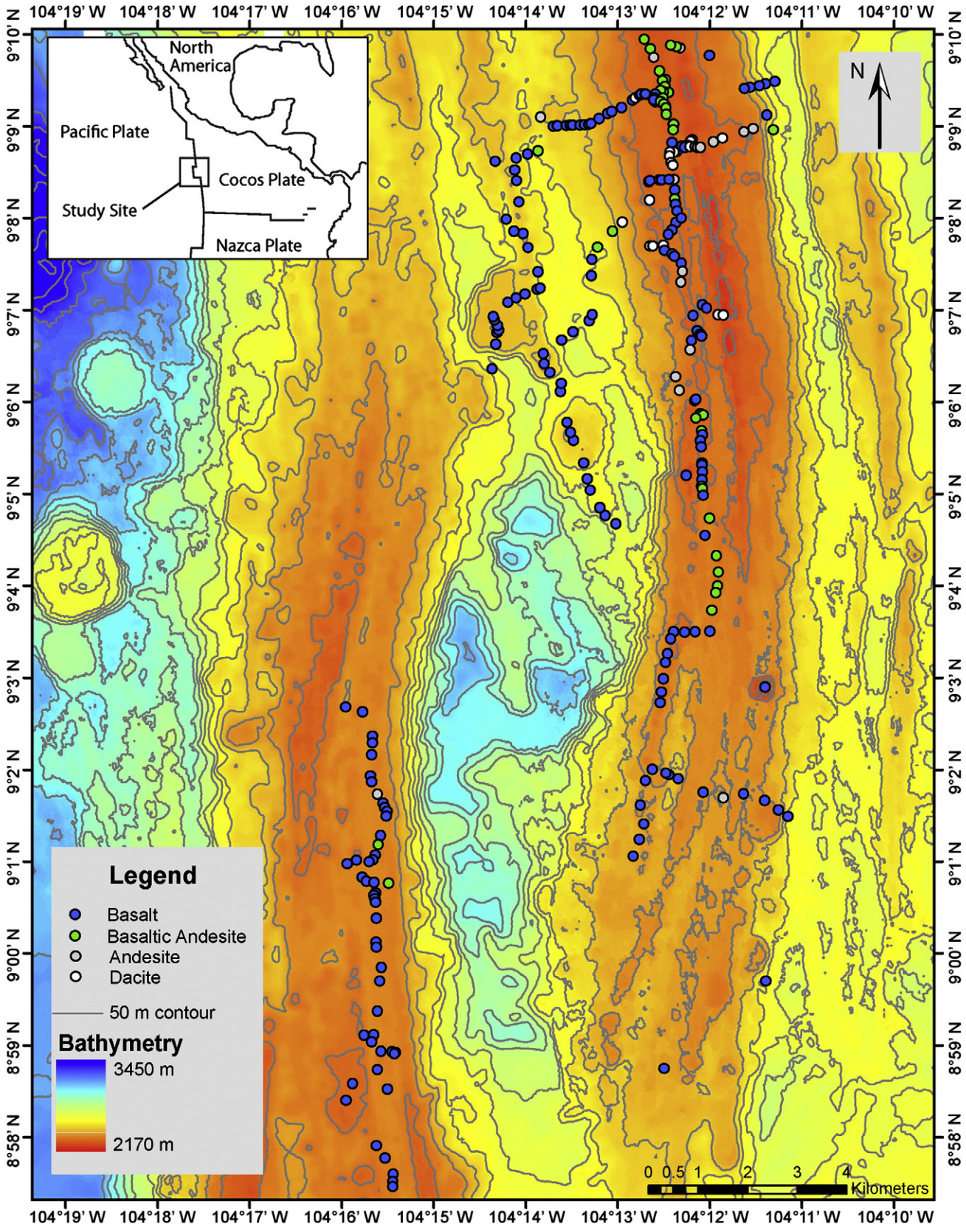

Fig. 1. Bathymetric map of the 9°N overlapping spreading center. Circles represent sample locations, with lighter colors representing lower MgO concentrations. The high-silica lavas are primarily confined to the eastern propagating limb, north of ~9°06′ N.
Bathymetric map modified from Wanless et al., 2010.

Please cite this article as: Wanless, V.D., et al., Volatile abundances and oxygen isotopes in basaltic to dacitic lavas on mid-ocean ridges: The role of assimilation at spreading centers, Chem. Geol. (2011), doi:10.1016/j.chemgeo.2011.05.017

crust (Michael and Schilling, 1989). They are thought to be a relatively common component of the upper ocean crust, though the composition and location within the crust remains largely unconstrained. Due to the limited stability of saline brines, it has been difficult to ascertain their exact compositions. However, they have relatively high concentrations of H_2O, NaCl, Sr, Ca, and K_2O (Berndt and Seyfreid, 1990; Von Damm et al., 1997) compared to MORB. The percent of NaCl in the brine may be highly variable, but up to 50% (30 wt.% Cl) has been estimated by measurements of fluid inclusions (Kelley and Delaney, 1987). Therefore, assimilation of brine material should increase Cl, Na_2O, and K_2O concentrations of the melt, although the exact mechanism of assimilation is not understood.

The bulk composition and mineralogy of altered crustal material may vary, depending on the temperature and pressure of alteration and the fluid/rock ratios (Alt et al., 1986). Constraints on the depth of assimilation come from studies of volatile concentrations in glasses (Michael and Cornell, 1998; le Roux et al., 2006) and textural observations in ophiolites (e.g. Gillis and Coogan, 2002), and are consistent with melting at the top of the shallow melt lens. The depth of the melt lens, however, may vary due to migration within crust over time and, therefore, the melt may interact with the upper gabbros and/or lower sheeted dikes (Gillis, 2008). If alteration is caused by circulation of hydrothermal fluids, it is likely that this is largely restricted by permeability to the base of the sheeted dikes and uppermost gabbros of Layer 3. This is also consistent with observations from drill cores from lower sheeted dikes and upper gabbros that have experienced low- to medium-grade metamorphism (up to greenschist or amphibolite facies; Alt et al., 1986; Coogan et al., 2003). Although hydrothermal circulation has little effect on the major element chemistry, the lower sheeted dikes and upper gabbros commonly show lower K_2O, Na_2O and $\delta^{18}O$ values, variable CO_2, higher H_2O and Cl concentrations (e.g. Alt et al., 1996) and slight S depletion (e.g. Alt et al., 1989) compared to the extrusive volcanic layer.

3. Analytical methods and results

3.1. Major and trace elements

During the *MEDUSA2007* research cruise, 275 glassy samples were collected from the 9°N OSC. Methods, standards and results from all major and trace element analyses are discussed in detail in Wanless et al. (2010) and are only briefly mentioned here. Glasses are fresh and primarily aphyric. Individual chips from each sample were handpicked to avoid any microphenocrysts and alteration. Major elements were analyzed on a JEOL 8900 Electron Microprobe at the USGS in Denver, Colorado. Each sample was analyzed 8 to 10 times and averages of these are reported here and in Wanless et al. (2010). The microprobe was calibrated using the USGS mineral standards and several in-house standards (JdF-D2, Reynolds, 1995; 2392-9, Smith et al., 2001; and USGS dacitic glass GSC) were used for secondary normalizations to account for instrumental drift (see Smith et al., 2001 for details). High-precision Cl, S and K_2O concentrations were determined using 200-second peak/100-second background counting times. The chlorine standard used was St 7820 Sodalite. Samples were analyzed for trace element concentrations on an Element2 Inductively Coupled Plasma Mass Spectrometer (ICP–MS) at the University of Florida (see Goss et al., 2010 for more analytical details). Concentration data and ratios used in this paper are listed in Table 1.

To simplify the discussion, we use the general terms "basalt and basaltic" to include basalts, ferrobasalts and FeTi basalts (<52 wt.% SiO_2). The intermediate lavas include both basaltic andesites and andesites, with SiO_2 concentrations that range from 52 to 57 wt.% and 57 to 62 wt.%, respectively. Dacites have >62 wt.% SiO_2. Cl concentrations range from 0.01 to 0.07 wt.% in the basalts and are systematically higher in the basaltic andesites (0.01 to 0.31 wt.%), andesites (0.20 to 0.42 wt.%) and dacites (0.23 to 0.70; Fig. 2). K_2O concentrations range from 0.13 to 1.37 wt.% and increase with increasing SiO_2 content. K_2O ranges from 0.13 to 0.21 wt.% in basalts, from 0.26 to 0.60 wt.% in basaltic andesites, from 0.63 to 0.83 wt.% in andesites and from 0.89 to 1.37 wt.% in dacites (Fig. 2). Although K_2O concentrations can be relatively high, all samples discussed here can be considered incompatible element depleted "normal" MORB (N-MORB) or their differentiates. Cl/K_2O ratios exhibit a marked increase from 0.04 to 0.60 with increased differentiation (Figs. 3 and 4). S concentrations range from 1898 to 345 ppm, with the highest concentrations observed in FeTi basalts and the lowest in the dacites (Fig. 5).

3.2. Volatile elements

A representative subset of 20 samples (covering the range of rock types) from the 9°N OSC was selected for volatile analyses (Table 1). Several glass chips were handpicked from each sample, avoiding alteration and microphenocrysts. Samples were analyzed for H_2O and CO_2 concentrations by Fourier transform infrared (FTIR) spectroscopy at the University of Oregon (Johnson et al., 2009). Water concentrations were calculated either using the fundamental OH stretching vibration at 3570 cm^{-1} or from the average of the two molecular water peaks (1630 cm^{-1} and 5200 cm^{-1}) and the 4500 cm^{-1} OH^- peak. An absorption coefficient of 63 L/mol cm was used for the 3570 cm^{-1} peak (Dixon et al., 1995a,b), and absorption coefficients for the near-IR peaks were calculated based on major element concentrations following methods in Mandeville et al. (2002). CO_2 concentrations were measured using the carbonate peaks at 1515 and 1430 cm^{-1}, using background subtraction procedures described in Johnson et al. (2009) and absorption coefficients calculated from Dixon and Pan (1995). The detection limit for CO_2 dissolved as carbonate is ~25 ppm. Dacite spectra were checked for molecular CO_2 (2350 cm^{-1}). In most cases, the concentrations were below the minimum detection limit of 2–5 ppm. In a few samples with excellent background characteristics, molecular CO_2 at the 1–2 ppm level was measured.

Volatile concentrations are highly variable but are generally consistent with major element trends (Table 1). H_2O concentrations range from 0.23 to 0.39 wt.% in basaltic glasses and from 0.24 to 1.56 in basaltic andesite samples (Fig. 2). Andesites have H_2O concentrations from 0.99 to 1.50 wt.% and dacites from 1.53 to 2.35 wt.%. CO_2 concentrations in basaltic glasses range from 131 to 256 ppm (Fig. 2). Two of the basaltic andesites had measurable CO_2 concentrations (232 and 184 ppm), but all others had CO_2 concentrations below the detection limit. Andesite and dacite CO_2 concentrations are also below the detection limit. H_2O/Ce ratios, which involve elements with similar magmatic incompatibility, generally increase with increasing silica (Fig. 3), with maximum values of 188 in basalts, 235 in basaltic andesites, 258 in andesites and 288 in dacites. H_2O/K_2O ratios vary from 0.095 to 2.59, with the highest ratios observed in the basaltic andesites (Fig. 4).

3.3. Oxygen isotope analyses and results

Oxygen isotope ratios ($\delta^{18}O$, per mil notation) of 26 fresh, microphenocryst-free glass chips, covering the range of rock types (Table 1), were determined at the CO_2-laser-fluorination laboratory at the University of Wisconsin, Madison, following methods described in Valley et al. (1995) and Spicuzza et al. (1998). Aliquots of 2.4–3.2 mg were treated with BrF_5 overnight, and then individually heated with a CO_2 laser in the presence of BrF_5. Measurements were standardized with 4–5 analyses of UWG-2 garnet standard per day ($\delta^{18}O = 5.8‰$; Valley et al., 1995), and are reported in standard δ-notation relative to Standard Mean Ocean Water (SMOW). Reproducibility of the standard during each session was better than ±0.15‰ (2SD).

Please cite this article as: Wanless, V.D., et al., Volatile abundances and oxygen isotopes in basaltic to dacitic lavas on mid-ocean ridges: The role of assimilation at spreading centers, Chem. Geol. (2011), doi:10.1016/j.chemgeo.2011.05.017

Table 1
Oxygen isotope, major and volatile element composition of lavas from the 9°N OSC.

Sample[a]	Depth (m)	SiO_2	TiO_2	Al_2O_3	FeO	MnO	MgO	CaO	Na_2O	K_2O	P_2O_5	Cl	S[b]	Tot H_2O[d]	CO_2[b,d]	$\delta^{18}O$	Ce[b]	Zr[b]	U[b]	La[b]	Cl/K_2O	H_2O/K_2O	H_2O/Ce	U/La
Basalts																								
264-04	2743	50.54	1.84	13.66	11.53	0.21	6.97	11.06	2.98	0.15	0.18	0.01	1477				15.5	142	0.09	5.0	0.09			0.018
264-08	2595	50.45	2.70	12.86	14.07	0.26	5.69	9.51	3.33	0.21	0.28	0.07	1898	0.39	231	5.79	20.5	180	0.13	6.8	0.35	1.82	188	0.019
265-17	2744	50.68	2.09	13.45	12.61	0.23	6.48	10.75	3.14	0.13	0.20	0.00	1607								0.03			
265-18	2701	50.75	1.82	14.01	11.31	0.21	7.21	11.26	2.97	0.12	0.18	0.01	1337	0.24	232		13.4	122	0.07	4.3	0.08	1.98	181	0.016
265-19	2724	50.62	1.83	14.02	11.23	0.21	7.19	11.24	2.93	0.12	0.18	0.01	1431								0.08			
265-20	2700	50.68	1.85	13.92	11.31	0.22	7.21	11.34	2.95	0.13	0.18	0.01	1319								0.09			
265-43	2587	50.12	1.92	13.86	11.57	0.21	6.83	11.13	2.81	0.13	0.19	0.01	1489	0.25	224		14.2	126	0.08	4.5	0.10	1.87	175	0.017
265-82	2529	50.77	1.95	13.81	11.70	0.22	6.93	11.21	2.69	0.14	0.19	0.01		0.24	256	5.51	13.0	123	0.08	4.1	0.07	1.74	185	0.019
265-88	2600	50.85	2.02	13.88	11.99	0.22	6.71	11.06	2.85	0.15	0.21	0.02		0.26	131	5.71	15.0	133	0.08	4.9	0.13	1.72	173	0.017
266-51	2592	50.55	1.94	13.85	11.59	0.21	7.33	10.97	2.86	0.13	0.19	0.01		0.23	218		13.3	144	0.08	4.2	0.09	1.82	172	0.019
265-104	2597	51.25	1.90	13.79	11.65	0.22	6.90	10.59	3.00	0.16	0.22	0.05		0.31	219		16.9	164	0.11	5.4	0.29	1.91	183	0.020
Basaltic andesites																								
264-10	2585	55.00	1.62	13.34	10.23	0.19	5.27	8.76	3.56	0.43	0.21	0.12	1182								0.28			
265-48	2587	53.85	2.36	13.06	13.33	0.24	4.44	8.36	3.57	0.35	0.26	0.05	1682								0.14			
265-49	2573	52.81	1.78	14.00	11.09	0.21	5.98	10.03	3.23	0.27	0.20	0.04	1274				21.3				0.16			
265-50	2569	54.15	2.14	13.41	12.19	0.22	4.54	8.45	3.59	0.40	0.28	0.09	1316				80.0		0.84	28.0	0.21			0.030
265-106	2583	53.33	1.94	13.26	12.35	0.24	5.11	8.71	3.67	0.32	0.39	0.19		0.65	184	5.77	33.9	339	0.24	10.9	0.59	2.02	191	0.022
265-103	2598	56.50	2.01	12.33	13.74	0.26	2.74	6.45	3.77	0.52	0.65	0.30		1.24	b.d.l	5.73	60.4	671	0.36	19.6	0.58	2.38	205	0.018
265-91	2567	56.83	2.10	12.31	14.23	0.28	2.09	6.24	3.45	0.60	0.78	0.31		1.56	b.d.l	5.31	66.1	724	0.39	21.4	0.52	2.59	235	0.018
265-125	2598	55.59	1.66	13.63	10.73	0.19	4.89	8.30	3.64	0.41	0.20					5.92	32.7		0.28	11.1	0.04			0.025
Andesites																								
265-90	2565	58.08	1.91	12.43	13.69	0.27	1.74	5.76	3.51	0.66	0.74	0.34		0.99	b.d.l		73.2	680	0.46	23.7	0.51	1.50	136	0.020
265-100	2591	58.09	1.76	12.64	12.68	0.24	1.89	5.51	3.82	0.63	0.54					5.56	72.7		0.45	23.7				0.019
266-54	2547	59.65	1.72	13.22	11.25	0.21	2.28	5.60	3.91	0.75	0.43	0.42		1.50	b.d.l	5.83	67.9	668	0.59	23.0	0.56	2.01	221	0.026
264-14	2580	61.75	1.30	13.46	8.71	0.17	2.47	5.54	3.94	0.83	0.22					6.06	57.0		0.51	19.4				0.026
265-69	2574	61.02	1.72	13.62	9.97	0.18	1.91	5.38	3.89	0.80	0.27	0.20		1.44	b.d.l		55.8	605	0.46	17.1	0.25	1.80	258	0.027
Dacites[c]																								
265-63	2591	64.43	1.29	13.26	8.22	0.15	1.29	4.21	3.71	0.99	0.21					5.57	68.1		0.59	23.5				0.025
265-64	2586	64.04	1.28	13.12	8.27	0.16	1.60	4.45	3.46	0.97	0.20	0.24		1.73	b.d.l	6.19	76.5	842	0.65	26.3	0.25	1.79	226	0.025
265-65	2576	63.79	1.26	13.25	8.14	0.15	1.34	4.21	3.84	0.97	0.22					5.86	67.5		0.59	23.3				0.025
265-66	2578	62.81	1.43	13.13	9.05	0.18	1.99	4.98	3.86	0.89	0.24	0.23		1.81	b.d.l	5.84	84.2	945	0.71	28.9	0.26	2.04	215	0.025
265-42	2586	66.92	0.94	13.09	8.04	0.17	0.86	3.49	0.83	1.17	0.21	0.51	427			5.87	82.9		0.91	29.0	0.44			0.031
265-67	2581	64.10	1.34	13.33	8.49	0.16	1.49	4.41	3.93	0.95	0.23					5.92	68.0		0.64	23.4				0.027
265-70	2567	66.26	0.87	13.20	7.17	0.14	0.80	3.23	4.08	1.33	0.19	0.70		2.35	b.d.l	6.08	88.1	934	1	30.9	0.53	1.76	266	0.034
265-83	2589	67.46	0.76	13.27	6.68	0.13	0.67	2.98	3.88	1.37	0.16	0.67		1.53	b.d.l	5.94	87.2	922	1.05	30.7	0.49	1.12	176	0.034
265-84	2601	64.39	1.13	13.17	8.18	0.15	1.23	3.92	3.41	1.19	0.22					5.73	77.8		0.82	27.3				0.030
265-85	2603	65.01	1.06	13.13	7.99	0.16	1.18	3.78	3.67	1.22	0.20	0.64		1.90	b.d.l	5.95	82.5	872	1	29.1	0.52	1.55	230	0.032
265-94	2528	65.22	0.97	13.04	7.90	0.14	1.13	3.54	4.29	1.14	0.23					5.90	83.9		0.84	29.1				0.029
265-95	2528	67.46	0.77	13.10	6.47	0.12	0.94	3.01	4.43	1.21	0.15					6.07	83.6		0.86	29.2				0.030
266-53	2550	64.28	1.06	13.31	8.06	0.14	1.12	3.73	4.16	1.09	0.25	0.66		1.74	b.d.l	5.38	82.2	856	0.86	28.5	0.60	1.60	211	0.030
266-57	2585	62.47	1.30	13.16	9.20	0.16	1.59	4.37	4.11	0.98	0.29	0.51		2.08	b.d.l	5.65	72.4	789	0.80	25.1	0.52	2.13	288	0.032
264-09	2571	65.97	0.90	13.19	7.02	0.13	1.05	3.47	4.32	1.20	0.21	0.58	345			5.73	83.9		1	29.0	0.48			0.034
In-house standard																								
2392-9		49.7	1.31	15.31	9.09	0.16	8.2	12.14	2.8	0.1	0.12	0.01	1337	0.15	165	5.48	8.9	80.6	0.05	2.8	0.10	1.50	169	0.018

Accuracy for these techniques is estimated to be ±10% for total H_2O and ±20% for CO_2 (Dixon and Clague, 2001).
[a] Major elements by electron microprobe and reported in wt.%.
[b] CO_2, S, Ce, Zr, U, and La concentrations reported in ppm.
[c] Dacite major and trace element concentrations from Wanless et al., 2010.
[d] Based on replicate analyses, precision (2s) for total H_2O is <16% (relative) and <11% for CO_2.

The $\delta^{18}O$ values range from 5.3 to 6.2‰ in the OSC lavas with an average of 5.79‰ (Fig. 6). The basalts and basaltic andesites have similar oxygen isotope ratios, from 5.51 to 5.79‰ and 5.31 to 5.92‰ respectively. The andesites and dacites have variable $\delta^{18}O$ (5.38 to 6.19‰), with a mean of 5.86‰.

4. Discussion

4.1. CO_2 and H_2O degassing

Both CO_2 and/or H_2O can undergo variable amounts of degassing during ascent from the magma chamber to eruption on the seafloor. Observations and experimental solubility data indicate that CO_2 degases more readily than H_2O in basaltic melts. Nonetheless, many MORB glasses are supersaturated with CO_2 at their submarine eruption depths (e.g., Dixon et al., 1988) indicating that the magma ascent rate is sufficiently rapid, the CO_2 diffusion rate is sufficiently slow, and the magmas quench rapidly upon eruption, which can inhibit CO_2 equilibration with the seafloor pressures. Therefore, in submarine settings, supersaturated CO_2 concentrations are often equated with the minimum depth of storage of the melt prior to eruption (e.g., Dixon et al., 1988). The depth of last equilibration of vapor-saturated melts can be calculated using the H_2O and CO_2 solubility model of Dixon et al. (1995a,b), which is calibrated on experimental results at pressures and temperatures similar to MOR magmatic conditions. Vapor saturation pressures for the OSC basaltic and evolved samples were calculated using the VolatileCalc program (Newman and Lowenstern, 2002), which utilizes experimental results and formulations of Dixon et al. (1995a,b). This program is calibrated for both high-silica and basaltic compositions and requires an input of

Please cite this article as: Wanless, V.D., et al., Volatile abundances and oxygen isotopes in basaltic to dacitic lavas on mid-ocean ridges: The role of assimilation at spreading centers, Chem. Geol. (2011), doi:10.1016/j.chemgeo.2011.05.017

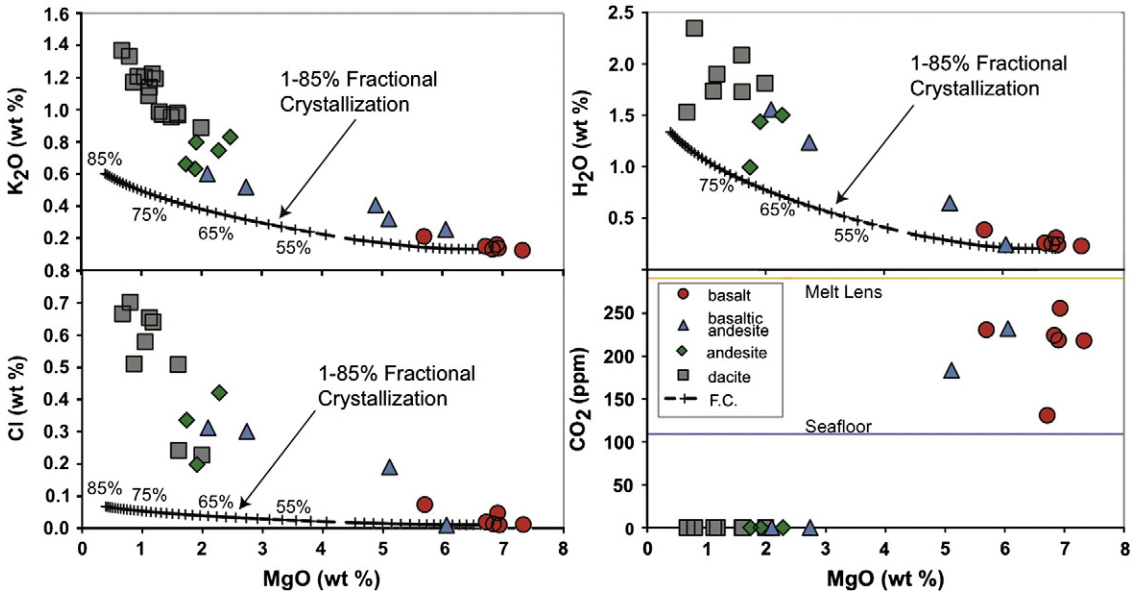

Fig. 2. K_2O (wt.%), H_2O (wt.%), Cl (wt.%), and CO_2 (ppm) versus MgO (wt.%) for glasses from the 9°N OSC. Black crosses indicate the calculated fractional crystallization trend using MELTS (Ghiorso and Sack, 1995). All dacitic lavas and several basaltic andesites lie above the calculated trend, indicating other processes are involved in their petrogenesis. K_2O and Cl diagrams modified from Wanless et al., 2010.

silica content (62 and 49 wt.% SiO_2, respectively) and temperature of the magma (900 and 1200 °C, respectively). Pressure estimates calculated using VolatileCalc are typically within ±10% of values calculated using other solubility models (Newman and Lowenstern, 2002).

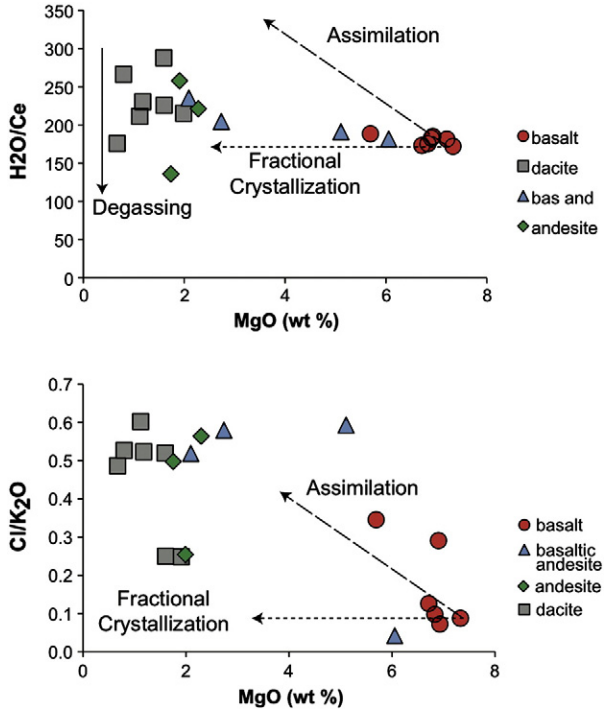

Fig. 3. H_2O/Ce and Cl/K_2O ratios versus MgO (wt.%) for glasses from the 9°N OSC. Generalized trends for assimilation and fractional crystallization are shown as straight dashed lines, although assimilation is likely to result in curved trends. In general, the andesites, dacites and most of the basaltic andesites have higher incompatible element ratios than the basaltic lavas, suggesting that they cannot result from fractional crystallization alone. Instead, they are consistent with assimilation of altered basalt. Low H_2O/Ce ratios are the result of variable degrees of H_2O degassing. The andesites/dacites with lower Cl/K_2O ratios (~0.24) were all collected from the same linear pillow mound that hosted the only observed active hydrothermal vent.

H_2O and CO_2 concentrations in the OSC lavas indicate a range of equilibration pressures with a maximum of ~550 bar (Fig. 7). Most of the basaltic lavas are supersaturated with CO_2 at their eruption depths, but they have equilibration pressures shallower than the top of the imaged melt lens (~1.5 km or 670 bar; Kent et al., 2000), suggesting some degassing occurred during ascent and eruption on the seafloor. The vapor saturation calculations are similar to those of previous studies of basalts on MOR, which show equilibration within or above the top of the imaged melt lens (e.g., le Roux et al., 2006). This is consistent with relatively high ascent rates of basaltic magmas at the OSC and limited degassing of CO_2 and H_2O.

In addition to completely degassing any initial CO_2 that they may have contained, more H_2O-rich magmas, like the OSC andesites and dacites, may degas some H_2O during ascent to the seafloor (Fig. 7). The high-silica lavas have equilibrium pressures, based on H_2O, that range from that of the seafloor (~250 bar) to ~500 bar, similar to the pressure calculated for basalts but somewhat lower than expected for the top of the melt lens. If we assume that the andesites and dacites formed in the melt lens, at pressures consistent with the base of the sheeted dikes (Wanless et al., 2010), then this range of H_2O concentrations suggests variable amounts of degassing during ascent and eruption on the seafloor. Degassing is consistent with the modest vesicularity of the high-silica lavas and correlates with lower H_2O/Ce ratios (Fig. 3).

H_2O is enriched in the crust during hydrothermal circulation (e.g. Alt et al., 1996) due to formation of secondary hydrous minerals, therefore elevated H_2O concentrations in fresh lavas may be an important signature of assimilation of altered crust. However, lower H_2O/Ce ratios (Fig. 3) and low CO_2 contents in the high-silica glasses suggest that magma degassing is an important process during storage, ascent and/or eruption. Therefore, using H_2O concentrations as a geochemical indicator of assimilation may be complicated by variable degrees of magma degassing prior to solidification on the seafloor.

4.2. Evidence for assimilation from trace elements

Liquid lines of descent (LLDs) calculations at fO_2 = QFM and P = 1 kbar (Wanless et al., 2010) suggest that fractional crystallization

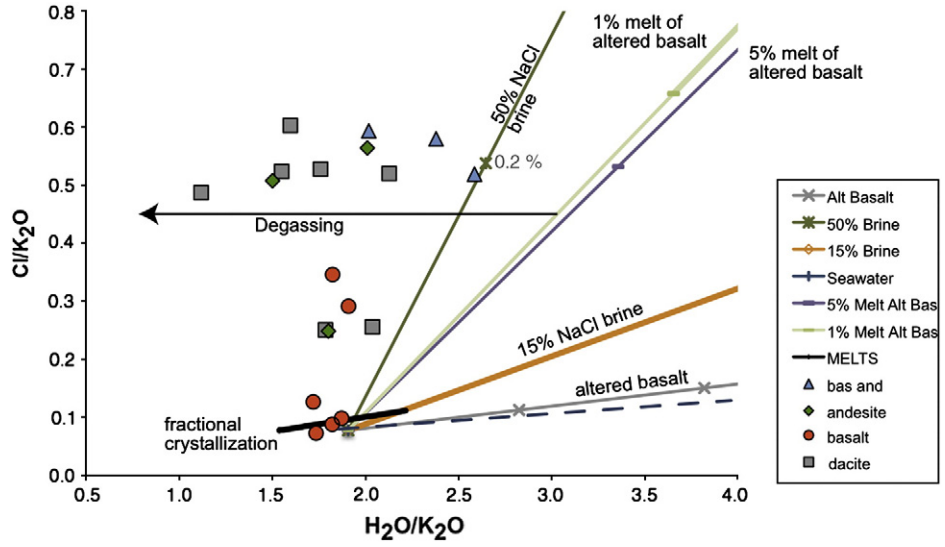

Fig. 4. Cl/K_2O versus H_2O/K_2O for glasses from the 9°N OSC. Lines representing mixing of 6 possible assimilants with an OSC basalt are shown. Mixing end-members include 1 and 5% partial melts of an altered basalt, an altered basalt, a 50% and 15% NaCl brine, and seawater (see text for references). Tick marks on the mixing lines denote the percent of each end-member from 1 to 100% by increments of 10. If less than 10% mixing is required, then no tick marks are shown. A 0.2 wt.% tick mark is shown for comparison in the case of 50% NaCl brine. See text for mixing end-member concentrations. A combination of partial melting of an altered basalt and <0.2 wt.% of a 50% NaCl brine with a basaltic end-member can explain the formation of high-silica lavas on the OSC, if H_2O has undergone variable amounts of degassing.

alone cannot account for the high Cl, K_2O, and H_2O concentrations observed in the MOR dacites, andesites or basaltic andesites (Fig. 2). H_2O concentrations in the dacites are as much as two times greater and Cl concentrations are more than ten times greater than model predictions (Fig. 2). H_2O/Ce ratios, which should not change over a wide range of anhydrous fractional crystallization, are generally higher in dacites and extend to values ~1.5 times higher than those of the basalts, whereas basaltic andesites and andesites show a range of ratios (Fig. 3). Cl/K_2O values, which increase during hydrothermal alteration but remain relatively constant during fractional crystallization, are as much as seven times higher in the dacites than values measured in the least evolved basalts (Fig. 3). Interestingly, the andesites and dacites with lower Cl concentrations and $Cl/K_2O<0.3$ were all recovered from a small pillow mound on-axis near the only active hydrothermal vent observed at the OSC, which suggests that the compositions of the assimilant may vary locally within the region.

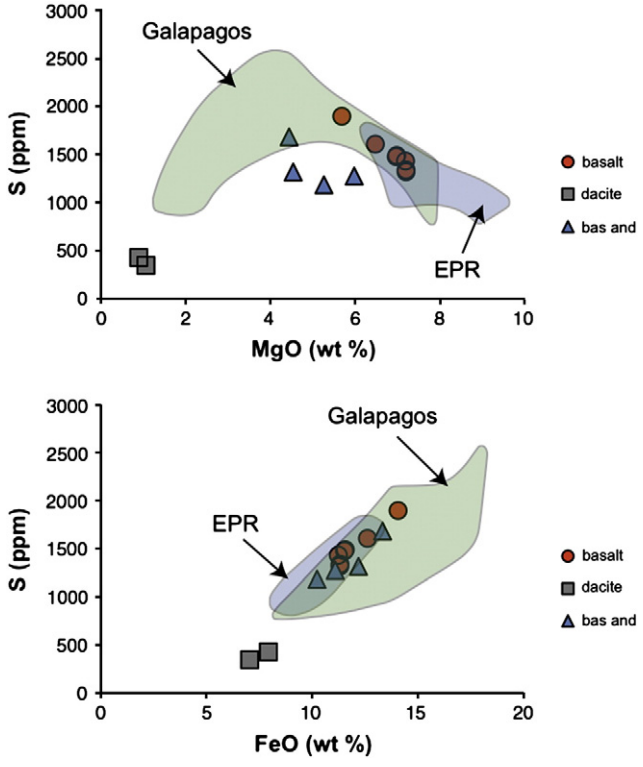

Fig. 5. S versus MgO and FeO for glasses from the 9°N OSC. MOR dacite glasses have low S contents, suggesting the formation of sulfides or degassing has occurred. Fields for lavas erupted at the Galapagos Spreading Center (Perfit et al., 1983) and EPR (le Roux et al., 2006) are also shown.

Altered crust is enriched in chlorine during hydrothermal circulation of seawater (Michael and Schilling, 1989) due to the incorporation of Cl into nominally hydrous minerals. Altered sheeted dikes can have a wide range of chlorine composition (49 to 647 ppm and a mean of 350 ppm) but these are generally higher than typical MORB concentrations (Sparks, 1995). The high Cl concentrations in the dacites are similar to model abundances produced by 1–15% partial melting of altered basalt crust (Wanless et al., 2010). Although both H_2O and Cl exhibit over-enrichments compared to calculated fractional crystallization trends (Fig. 2), the Cl over-enrichment is much greater than that of H_2O. Cl degassing is insignificant during most submarine eruptions, due to the elevated of pressures at the seafloor, (~250 bar) (Unni and Schilling, 1978; Webster et al., 1999). Therefore, the difference between these enrichment factors may be caused by variable amounts of H_2O degassing, as discussed above or alternatively, the assimilant may have much higher Cl/H_2O compared to the uncontaminated magma, resulting in more enriched Cl concentrations.

le Roux et al. (2006) used Cl/Nb ratios to assess the role of assimilation in MORB magmas because Cl and Nb have similar partition coefficients in basaltic systems and during seawater alteration these elements become decoupled, Cl being enriched in the altered material and Nb being immobile. Unfortunately, an added complication to using this approach is that advanced fractional crystallization in the OSC lavas results in precipitation of Fe–Ti oxides in which Nb is a compatible element. Consequently, the Cl/Nb ratio changes and cannot be used as an alteration discriminant when high-silica lavas are involved. Here, we use Cl/K_2O (Fig. 3) because these elements also have broadly similar incompatibilities over a wide range of crystallization (e.g., Kent et al., 1999), and this ratio has been used in several studies to identify crustal contamination (e.g., Michael and Cornell, 1998; Kent et al., 1999). The siliceous lavas at the OSC

Please cite this article as: Wanless, V.D., et al., Volatile abundances and oxygen isotopes in basaltic to dacitic lavas on mid-ocean ridges: The role of assimilation at spreading centers, Chem. Geol. (2011), doi:10.1016/j.chemgeo.2011.05.017

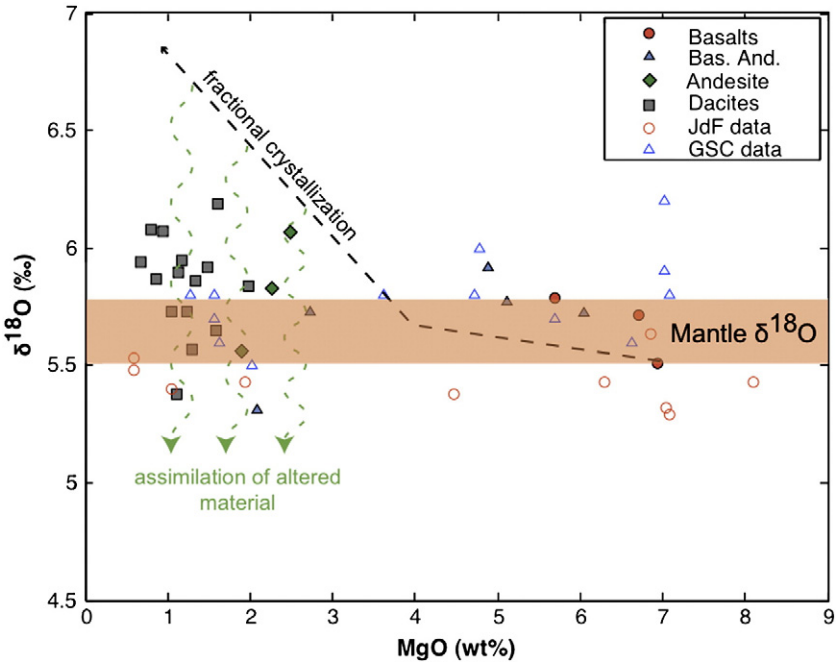

Fig. 6. $\delta^{18}O$ versus MgO for glasses from the 9°N OSC. The MOR dacites, andesites and several basaltic andesites lie below calculated fractional crystallization trends (black dashed line). The lower $\delta^{18}O$ values are consistent with assimilation of altered oceanic crust, which has lower $\delta^{18}O$ values due to high-temperature hydrothermal circulation. $\delta^{18}O$ values for lavas from the Juan de Fuca ridge and Galapagos Spreading Center are shown for comparison.

have Cl/K_2O ratios three to seven times greater than the values observed in spatially related basalts (Fig. 3) and significantly higher than maximum mantle values (0.065) suggested by Michael and Cornell (1998). The elevated Cl abundances and incompatible element ratios in the evolved lavas therefore suggest they have been contaminated by crustal material and are consistent with assimilation of altered crust coupled with fractional crystallization (AFC) (Wanless et al., 2010). AFC processes will also produce an increase in incompatible trace element concentrations, particularly in elements enriched during seawater alteration, such as U (Wanless et al., 2010). This is evident in variations in U/La ratios, which are not affected by fractional crystallization but will increase due to assimilation of altered basalt (Fig. 8). These observations clearly indicate the operation of assimilation in the formation of basaltic andesites, andesites and dacites on MOR.

4.3. Evidence for assimilation from oxygen isotopes

Fractional crystallization of Fe–Ti oxides leads to an increase in $\delta^{18}O$ values of evolving magmas (Taylor, 1968) because these phases, and to a lesser extent Fe–Mg silicates, preferentially incorporate ^{16}O relative to ^{18}O (Taylor, 1968; Anderson et al., 1971; Muehlenbach and Byerly, 1982). During crystallization of MORB magma there is a slight increase in $\delta^{18}O$ as the magma crystallizes ferromagnesian silicates, followed by a more rapid increase when Fe–Ti oxides precipitate (Matsuhisa et al., 1973). Thus, advanced fractional crystallization should result in an increase of $\delta^{18}O$ values by 0.5–1.5‰ in dacitic lavas (Bindeman, 2008, e.g., Muehlenbach and Byerly, 1982).

Using modal mineral proportions calculated from MELTS (Ghiorso and Sack, 1995) and oxygen isotope fractionation factors from Bindeman (2008), we calculated the change in $\delta^{18}O$ during fractional

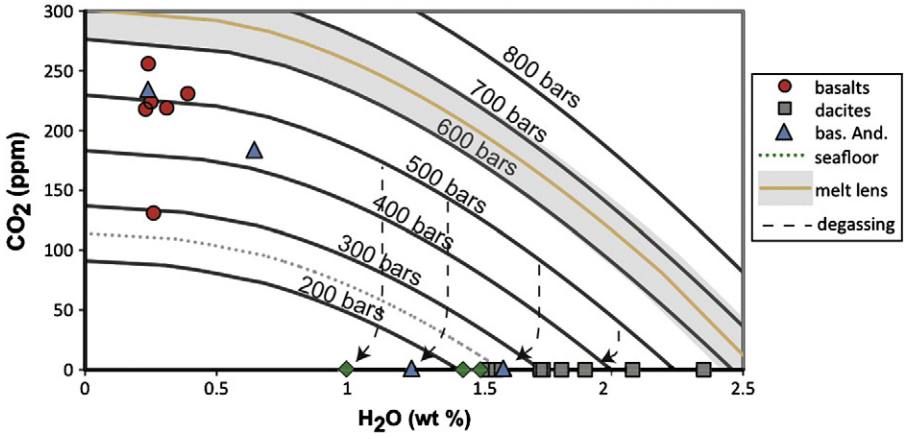

Fig. 7. H_2O versus CO_2 for 9°N OSC glasses. Superimposed on this diagram are CO_2–H_2O vapor saturation curves for 200 to 800 bar based on models by Dixon et al. (1995a, b). Black dashed lines show a general magma degassing trends during ascent. The gray band represents an approximate depth of the top of the imaged melt lens (Kent et al., 2000). The pressure at the seafloor is shown as a dotted line. Most of the basalts are in equilibrium with pressures shallower than the top of the imaged melt lens (~670 bar). The dacites, andesites, and two basaltic andesites have completely degassed CO_2 and may have also lost H_2O prior to or during eruption. H_2O and CO_2 concentrations in one basaltic andesite lie between the high-silica lavas and the basaltic lavas.

Please cite this article as: Wanless, V.D., et al., Volatile abundances and oxygen isotopes in basaltic to dacitic lavas on mid-ocean ridges: The role of assimilation at spreading centers, Chem. Geol. (2011), doi:10.1016/j.chemgeo.2011.05.017

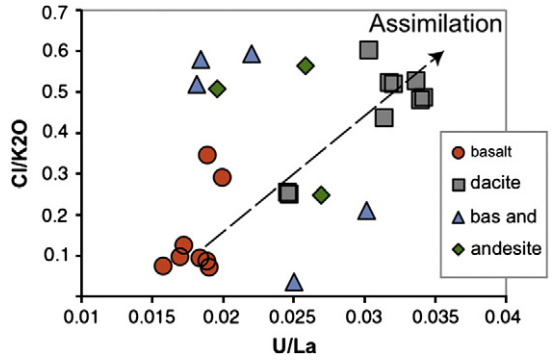

Fig. 8. Cl/K_2O versus U/La. Elevated Cl/K_2O values of the high-silica lavas can be explained by assimilation of altered crustal material that is enriched in Cl, and U compared to K_2O and La during seawater alteration. Several OSC basaltic lavas have elevated Cl/K_2O values, suggesting assimilation may also be important in their petrogenesis.
U and La data from Wanless et al., 2010.

crystallization of a MORB parental magma (Fig. 6). If the MOR dacites had formed through fractional crystallization, the $\delta^{18}O$ should be ~6.8‰, but the measured ratios are ~1‰ lower (dacite average = 5.84‰), supporting the conclusion that the dacites could not exclusively form by fractional crystallization. Low values ($\delta^{18}O$ = 3.9–6.2‰) have also been observed in dacites erupted at the Galapagos Spreading Center (Perfit et al., 1999).

The temperature-dependent fractionation of oxygen isotopes between seawater ($\delta^{18}O = 0$) and primary magmatic minerals (e.g., $\delta^{18}O$ ~5.2–6.1‰ for olivine, clinopyroxene, and plagioclase) causes a bulk decrease in $\delta^{18}O$ of ocean crust during high-temperature hydrothermal alteration, but increases the $\delta^{18}O$ during low-temperature alteration (<200–250 °C; Alt et al., 1996; Muehlenbach and Clayton, 1972). In the latter case, the fluid evolves to lower $\delta^{18}O$ values in a closed system due to mass balance. This effect, together with the increase in temperature with depth, is obvious in profiles of oxygen isotope ratios in exposed sections of fast-spreading ocean crust (Hess Deep; Agrinier et al., 1995; Gillis et al., 2001) and drill holes (e.g., ODP Site 504; Alt et al., 1996). $\delta^{18}O$ values are higher than unaltered MORB compositions (~5.6 ± 0.2‰; Eiler, 2001) in the upper volcanic section of the crust but decrease to lower than mantle values in the lower sheeted dikes and gabbros (for profiles see Alt and Teagle, 2000).

The $\delta^{18}O$ of the sheeted dike and gabbro layers is quite variable but the sheeted dikes at Hess Deep have an average value of 5.1‰ (Gillis et al., 2001) and are as low as 2.9‰ (Agrinier et al., 1995), significantly different than mantle values of 5.6‰ (e.g., Alt et al., 1986; Eiler, 2001). Bulk melting of surrounding wall rock will result in $\delta^{18}O$ values similar to the altered whole rock values, however, partial melts in equilibrium with the altered basalts will have oxygen isotope ratios generally less than mantle-equilibrated values, but higher (by ~1‰; e.g., Muehlenbach and Byerly, 1982) than the altered basalt itself. Assimilation of these partial melts into fractionating magma will produce melts with oxygen isotope ratios between those of altered basalt and that expected from fractional crystallization alone. The $\delta^{18}O$ value of the MOR andesites and dacites range from 5.38 to 6.19‰, which is much more variable than the spatially related basalts and lower than values predicted by fractional crystallization (Fig. 6).

Taylor (1968) suggested that to a first approximation, the effect of assimilation on oxygen isotope ratios can be determined using mass balance equations. Using results from Energy Constrained-Assimilation and Fractional Crystallization (EC-AFC) petrologic modeling calculations (Bohrson and Spera, 2001), which, unlike traditional AFC models, includes energy conservation in the formulation, the ratio of fractionating magma to partially melted assimilant (M_f/M_a) in the dacites is ~2.5:1 to 3.5:1 (Wanless et al., 2010). Using this range of ratios and assuming the evolved magma has a $\delta^{18}O$ of 6.8‰ (largely due to fractionation of Fe–Mg silicates and iron oxides) and an assimilant with a $\delta^{18}O$ of 3.4‰ to 5.6‰ (from partial melting of an altered basalt with a $\delta^{18}O$ of 2.9‰ to 5.1‰), the oxygen isotope ratio of the resultant magma would range from 5.8‰ to 6.5‰. This range includes the average ratios observed in the dacites and is less than predicted solely as a consequence of crystal fractionation. Varying the ratio of the fractionated magma to assimilant (M_f/M_a of 2:1 to 4:1) or the $\delta^{18}O$ value of the assimilant (from 2.9‰ to 6‰) can produce a range of compositions in the resulting magma (Fig. 9). To produce the lowest values observed at the OSC the assimilant must have a $\delta^{18}O$ value of less than 4‰ or the M_f/M_a must be lowered. Assuming the assimilated altered crust has the lowest $\delta^{18}O$ value observed at Hess Deep of 2.9‰ (Agrinier et al., 1995) the range of $\delta^{18}O$ values produced by AFC is 5.6‰ to 5.9‰, assuming M_f/M_a values from 2.5 to 3.5:1. If instead, the M_f/M_a ratio is lowered to 2:1, than $\delta^{18}O$ values of 5.4‰ can be produced. Therefore, either increasing the amount of assimilant relative to fractionating magma or lowering the $\delta^{18}O$ value of the assimilant can produce the range of $\delta^{18}O$ values observed in dacites at the OSC.

4.4. Potential sources of assimilant

Despite growing evidence of crustal contamination on MORs, the nature of the assimilant and depth of the process remain poorly constrained, although some potential candidates can be eliminated if several geochemical parameters are considered. As mentioned above, Cl/K_2O and H_2O/K_2O ratios provide a means to discriminate between sources of contamination on MOR because of the variable concentrations of these elements in possible assimilants (Kent et al., 1999). Potential contaminants on MOR include:

1) Altered basaltic crust: Cl = 0.35 wt.% (Sparks, 1995); H_2O = 1.3 wt.% (Agrinier et al., 1995); K_2O = 0.08 wt.% (Stewart et al., 2002);
2) Seawater: Cl = 1.935 wt.%, H_2O = 97.5 wt.%, K_2O = 0.04 wt.%; (Kent et al., 1999);
3) Saline brines of variable compositions, for example: 15% NaCl brine (Cl = 9.9 wt.%, H_2O = 85 wt.%, K_2O = 0.25 wt.%); and 50% NaCl brine (Cl = 30.3 wt.%, H_2O = 50 wt.%, K_2O = 0.25 wt.%; Kent et al., 1999 and references therein for brine compositions);
4) Low-degree partial melts of altered ocean crust that have a range of compositions with relatively low MgO, and high Cl, H_2O and K_2O (Wanless et al., 2010).

Bulk mixing of altered basaltic crust or seawater with OSC basalt cannot produce the observed compositions of the MOR dacites (Fig. 4). Mixing of saline brines or partial melts of altered crust can explain the elevated Cl/K_2O ratios observed in the dacites, but is not consistent with the observed low H_2O/K_2O ratios of the dacites, (Fig. 4), although the latter is likely influenced by H_2O degassing. While discrimination between these two possible assimilants (brines versus crust) is difficult, only assimilation of altered ocean crust is consistent with major and trace element concentrations and petrologic modeling of MOR dacites (Wanless et al., 2010). Additionally, although le Roux et al. (2006) suggested that EPR MORB magmas were contaminated with brine at depths below the lava/dike (seismic layer 2A/2B) boundary and above the axial melt lens (~1400 m below seafloor) there is no consensus on the depth of brine formation or loci of storage at active ridges and therefore it is uncertain if saline brines are actually present within the zone of assimilation. Low Cl fluids may exist within the altered ocean crust but are not considered here because the high-Cl concentrations of the dacites makes this source of contamination unrealistic. Therefore, partially melted altered crust is the most likely source of contamination observed in the high-silica magmas and the low H_2O/K_2O ratios in the dacites results from degassing.

Please cite this article as: Wanless, V.D., et al., Volatile abundances and oxygen isotopes in basaltic to dacitic lavas on mid-ocean ridges: The role of assimilation at spreading centers, Chem. Geol. (2011), doi:10.1016/j.chemgeo.2011.05.017

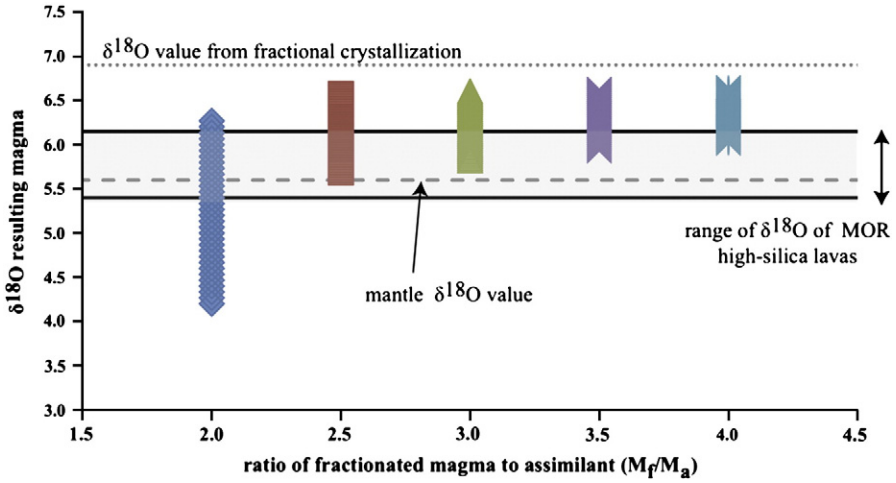

Fig. 9. Diagram showing the range of oxygen isotope compositions that can be produced from varying the ratio of fractionated magma to assimilated material (M_f/M_a) in AFC calculations. The $\delta^{18}O$ value of the resulting magma was calculated for ratios of 2:1, 2.5:1, 3:1, 3.5:1, and 4:1 using assimilants with a range of $\delta^{18}O$ values similar to those observed in altered sheeted dikes (2.9–6‰). M_f/M_a values from 2 to 4 can produce $\delta^{18}O$ values similar to MOR dacites but lower values of M_f/M_a (2–2.5) are required to explain the lowest $\delta^{18}O$ observed at the OSC. Small dotted line shows the $\delta^{18}O$ value of magmas produced from fractional crystallization alone. Dashed line shows the mantle $\delta^{18}O$ value.

4.5. Sulfur in MOR dacites

Sulfur concentrations in the dacites are low (345 to 427 ppm) compared to those of basalts and basaltic andesites (Fig. 5), which is consistent with the relatively low S levels observed in high-silica lavas erupted at other ridges (Perfit et al., 1983). Possible explanations for the low S concentrations include fractional crystallization, formation of immiscible sulfide (Fe–S–O) liquid, magma mixing, assimilation, degassing, or some combination of the above. Sulfur concentrations increase in MORB magmas during fractional crystallization as FeO increases until the melt becomes saturated with respect to Fe-oxides, after which S contents decrease dramatically along with FeO (Mathez, 1976; Wallace and Carmichael, 1992). The decrease in S observed in the OSC andesites and dacites, which correlates with the decrease in FeO, likely results from the low S solubility caused by decreasing FeO contents and decreasing temperature of the melt (Wallace and Carmichael, 1992). These factors lead to separation of a sulfide phase (Perfit et al., 1999). Nearly all MORB glasses are saturated with immiscible Fe–S–O liquid (Wallace and Carmichael, 1992). In the range from basalt to FeTi basalt, S does not increase nearly as much as would be expected if it were a highly incompatible element, implying that S content is being moderated by a sulfide phase. Lower S contents in andesites from the Galapagos Spreading Center are thought to result from the formation and fractionation of these immiscible monosulfide liquids (Perfit et al., 1999). Bulk assimilation may also contribute to lower S concentrations in the resulting melt, as altered sheeted dikes have lower S concentrations than typical MORB magmas (e.g. Alt et al., 1989), but low degree partial melts of the altered dikes have variable S contents depending on the degree of melting and the S concentration of the assimilant. Finally, degassing may cause a decrease in S in the melt phase during transport to and eruption on the seafloor (e.g., Perfit et al., 1983, 1999). Therefore, while assimilation of altered material may produce lower S concentrations, sulfur is not a useful discriminator of assimilation due to the numerous processes that affect its concentrations.

4.6. Formation of oceanic plagiogranites

Plagiogranites are volumetrically small but ubiquitous siliceous components of the ocean crust and have been observed as veins and small intrusions in ophiolites (e.g. Pedersen and Malpas, 1984), in deep drill cores from the ocean crust (e.g. Casey, 1997; Dick et al., 2000), and as xenoliths in Icelandic lavas (Sigurdsson, 1977). There are also many examples of evolved plutonic rocks from slower spreading centers (e.g. Mid-Atlantic Ridge; Aumento, 1969, Southwest Indian Ridge; Dick et al., 2000). The origin of these veins and intrusions remains unclear but two main, non-exclusive hypotheses are: 1) partial melting of gabbroic crust (e.g. Koepke et al., 2004, 2007) and 2) extreme crystal fractionation of tholeiitic magmas (Beccaluva et al., 1999; Coleman and Donato, 1979; Niu et al., 2002).

The composition of oceanic plagiogranites varies considerably (Koepke et al., 2007), making a direct petrologic comparison with the MOR dacites difficult. However, trace element concentrations in the MOR dacites (Wanless et al., 2010) and the most evolved plagiogranite ($SiO_2 = 63$ wt.%) vein from the mid-Atlantic Ridge (Godard et al., 2009) are quite distinct, suggesting that the MOR dacites are not simply the extrusive equivalents of plagiogranite veins. For example, trace element enrichments observed in the MOR dacites (e.g. 1050 ppm Zr; 17 ppm Nb; 160 ppm Y) are much greater than those of the plagiogranite veins (e.g. 328 ppm Zr; 9.7 ppm Nb; 142 ppm Y). Also, although plagiogranite veins have positive Zr and Hf anomalies, they lack the negative Nb and Ta and elevated U and Th concentrations observed in MOR dacite glasses (Wanless et al., 2010). These variations in trace element patterns likely reflect differences in processes involved in the formation of these high-silica rocks. MOR dacites require both extensive fractional crystallization and assimilation of altered crustal material, while some plagiogranite veins may simply be the result of partial melting of unaltered ocean crust.

Zircons from plagiogranite veins can also have variable oxygen isotope ratios. Uniform mantle-like $\delta^{18}O$ values of zircons collected from plagiogranite veins in the gabbroic crust at the mid-Atlantic and southwest Indian ridges (~5.2 ± 0.5‰) require no seawater contamination in the evolved melt at these depths (Grimes et al., 2011), but lower $\delta^{18}O$ values in plagiogranite veins from the Oman ophiolite (average of 4.6 ± 0.6‰) are thought to represent remelting of ocean crust that had been altered with respect to oxygen isotopes at high temperatures (Grimes et al., 2010). These studies suggest that high-silica lavas can form in a variety of different MOR settings and may have a range of compositions but that crustal melting is an important process in their petrogenesis.

5. Conclusions

Oxygen isotope values and volatile concentrations suggest the MOR dacites form by a combination of assimilation and fractional crystallization. Fast ascent rates for basaltic magmas from the 9°N OSC

Please cite this article as: Wanless, V.D., et al., Volatile abundances and oxygen isotopes in basaltic to dacitic lavas on mid-ocean ridges: The role of assimilation at spreading centers, Chem. Geol. (2011), doi:10.1016/j.chemgeo.2011.05.017

are required because the erupted lavas are supersaturated with CO_2. In contrast, high-silica lavas have completely degassed any initial CO_2, and variably degassed H_2O prior to eruption and have relatively low H_2O/K_2O ratios. These characteristics may result from slower ascent rates and/or lower effusion rates of high-silica magmas, and are consistent with the presence of large elongate vesicles and large extrusive pillow forms.

Volatile concentrations and $\delta^{18}O$ in 9°N OSC lavas suggest crustal assimilation was a common process during their petrogenesis. Although evidence of assimilation in the 9°N OSC basalts is limited, more extreme signatures of assimilation are observed in high-silica andesites and dacites. This is consistent with previous petrogenetic models based on major and trace element studies (Wanless et al., 2010) that show chemical variations cannot be explained by fractional crystallization alone. Even though some volatile degassing is likely to have occurred during eruption of the high-silica lavas, H_2O concentrations are up to two times higher in dacitic lavas compared to those expected based on calculated fractional crystallization trends, whereas Cl has excesses of seven to ten times predicted values. $\delta^{18}O$ values are on average ~1‰ lower than ratios expected from fractional crystallization of ferromagnesian silicates and Fe–Ti oxide phases, consistent with assimilation of an additional component or components. The range in $\delta^{18}O$ values can be explained by assimilation of oceanic crust altered to various degrees or by changing the ratio of the mass of fractionated magma to the mass of an assimilant with relatively low $\delta^{18}O$ values.

Our chemical and isotopic data are most consistent with the partially melted, hydrothermally-altered oceanic crust as the source of the contamination. However, the involvement of small volumes of saline brines, produced during two-phase separation of high-temperature hydrothermal fluids, cannot be discounted. Vapor saturation pressures calculated from H_2O–CO_2 data suggest that assimilation most likely occurs above the top of the seismically-imaged melt lens, which at the 9°N OSC, corresponds approximately to the base of the sheeted dikes.

Acknowledgments

We thank the captain, officers and crew of the R/V Atlantis for all their help during cruise AT15-17, the MEDUSA2007 Science party (including S. White, K. Von Damm, D. Fornari, A. Soule, S. Carmichael, K. Sims, A. Zaino, A. Fundis, J. Mason, J. O'Brien, C. Waters, F. Mansfield, K. Neely, J. Laliberte, E. Goehring, and L. Preston) for their diligence in collecting data and samples for this study. We thank the Jason II shipboard and shore-based operations group for their assistance in collecting these data and HMR for processing all DSL-120 sidescan and bathymetry collected during this cruise. Special thanks to J. W. Valley and the Stable Isotopes Lab at the University of Wisconsin—Madison for oxygen isotope analyses and thoughtful discussion throughout the preparation of this manuscript. Thanks to G. Kamenov and the UF Center for Isotope Geoscience for laboratory assistance. This manuscript benefited greatly from thoughtful and detailed reviews by Peter Michael and an anonymous reviewer. This research was supported by the National Science Foundation (grants OCE-0527075 to MRP, OCE-0526120 to EMK, EAR-0509639, 0838058 to JWV for laser fluorination) and the Department of Energy (grant 93ER14389 to JWV).

References

Agrinier, P., Hekinian, R., Bideau, D., Javoy, M., 1995. O and H stable isotope compositions of oceanic crust and upper mantle rocks exposed in the Hess Deep near the Galapagos Triple Junction. Earth and Planetary Science Letters 136, 183–196.

Hydrothermal Alteration and Fluid Fluxes in Ophiolites and Oceanic Crust. In: Alt, J., Teagle, D.A.H. (Eds.), Geological Society of America, Boulder, CO. 273–297 pp.

Alt, J., Honnorez, J., Laverne, C., Emmerman, R., 1986. Hydrothermal alteration of a 1 km section through the upper oceanic crust, deep sea drilling project hole 504B: mineralogy, chemistry, and evolution of seawater–basalt interactions. Journal of Geophysical Research 91, 10,309–10,335.

Alt, J., Anderson, A.T., Bonnell, L., 1989. The geochemistry of sulfur in a 1.3 km section of hydrothermally altered oceanic crust, DSDP Hole 504B. Geochemica et Cosmochimica Acta 53, 1011–1023.

Alt, J., Laverne, C., Vanko, D.A., Tartarotti, P., Teagle, D.A.H., Bach, W., Zuleger, E., Erzinger, J., Honnorez, J., Pezard, P., Becker, K., Salisbury, M.H., Wilkens, R.H., 1996. Hydrothermal Alteration of a Section of Upper Oceanic Crust in the Eastern Equatorial Pacific: A Synthesis of Results from Site 504 (DSDP Legs 69, 70, and 83, and ODP Legs 111, 137, 140, and 148). Proceedings of the Ocean Drilling Program, Scientific Results 148, 417–434.

Anderson, A.T., Clayton, R.N., Mayeda, T.K., 1971. Oxygen isotope thermometry of mafic igneous rocks. Journal of Geophysical Research 85, 715–729.

Aumento, F., 1969. Diorites from the mid-Atlantic ridge at 45°N. Science 165, 1112–1113.

Batiza, R., Niu, Y., 1992. Petrology and magma chamber processes at the East Pacific Rise 9°30′N. Journal of Geophysical Research 97, 6779–6797.

Bazin, S., Harding, A.J., Kent, G.M., Orcutt, J.A., Tong, C.H., Pye, J.W., Singh, S.C., Barton, P.J., Sinha, M.C., White, R.S., Hobbs, R.W., Van Avendonk, H.J.A., 2001. Three-dimensional shallow crustal emplacement at the 903′ N overlapping spreading center on the East Pacific Rise: correlations between magnetization and tomographic images. Journal of Geophysical Research 106, 16,101–16,117.

Beccaluva, L., Chinchilla-Chaves, A.L., Coltorti, M., Giunta, G., Siena, F., Vaccaro, C., 1999. Petrological and structural significance of the Santa Elena-Nicoya ophiolitic complex in Costa Rica and geodynamic implications. Contributions to Mineralogy and Petrology 11, 1091–1107.

Berndt, M.E., Seyfreid, W.E.J., 1990. Boron, bromine, and other trace elements as clues to the fate of chlorine in mid-ocean ridge vent fluids. Geochemica et Cosmochimica Acta 54, 2235–2245.

Bindeman, I.N., 2008. Oxygen isotopes in mantle and crustal magmas as revealed by single crystal analysis. Reviews in Mineralogy and Geochemistry 69, 445–478.

Bohrson, W.A., Spera, F., 2001. Energy-constrained open-system magmatic processes II: application of energy constrained assimilation-fractional crystallization (EC-AFC) model to magmatic systems. Journal of Petrology 42, 1019–1041.

Carbotte, S.M., Macdonald, K.C., 1992. East Pacific Rise 8°–10°30′N: evolution of ridge segments and discontinuities from SeaMARC II and three-dimensional magnetic studies. Journal of Geophysical Research 97, 6959–6982.

Casey, J.F. (Ed.), 1997. Comparison of Major- and Trace-element Geochemistry of Abyssal Peridotites and Mafic Plutonic Rocks with Basalts from the MARK Region of the Mid-Atlantic Ridge. Ocean Drilling Program, College Station. 181–241 pp.

Christie, D.M., Sinton, J.M., 1981. Evolution of abyssal lavas along propagating segments of the Galapagos Spreading Center. Earth and Planetary Science Letters 56, 321.

Coleman, R.G., Donato, M.M., 1979. Oceanic plagiogranite revisited, in Barker, F., ed., Trondhjemites, dacites and related rocks: Developments in Petrology 6: Amsterdam, Elsevier, pp. 149–168.

Coogan, L.A., 2003. Contaminating the lower crust in the Oman ophiolite. Geology 31, 1065–1068.

Coogan, L.A., Mitchell, N.C., O'Hara, M.J., 2003. Roof assimilation at fast spreading ridges: an investigation combining geochemical, and field evidence. Journal of Geophysical Research 108, 1–14.

Detrick, R.S., Buhl, P., Vera, E., Mutter, J., Orcutt, J.A., Madsen, J., Brocher, T., 1987. Multichannel seismic imaging of a crustal magma chamber along the East Pacific Rise. Nature 326, 35–41.

Dick, J.B., Natland, J.H., Alt, J., Bach, W., Bideau, D., Gee, J.S., Haggas, S., Hertogen, J.G.H., Hirth, G., Holm, P.M., Ildefonse, B., Iturrino, G.J., John, B.E., Kelley, D.S., Kikawa, E., Kingdon, A., le Roux, P.J., Maeda, J., Meyer, P.S., Miller, D.J., Naslund, H.R., Niu, Y., Robinson, P.T., Snow, J., Stephen, R.A., Trimby, P.W., Worm, H.U., Yoshinobu, A., 2000. A long in situ section of the lower ocean crust: results of ODP Leg 176 drilling at the Southwest Indian Ridge. Earth and Planetary Science Letters 179, 31–51.

Dixon, J.E., Pan, V., 1995. Determination of the molar absorptivity of dissolved carbonate in basanitic glass. American Mineralogist 80, 1339–1342.

Dixon, J.E., Clague, D.A., 2001. Volatiles in Basaltic Glasses from Loihi Seamount, Hawaii: Evidence for a Relatively Dry Plume Component. Journal of Petrology 42, 627–654.

Dixon, J.E., Stolper, E.M., Delaney, J.R., 1988. Infrared spectroscopic measurements of CO2 and H2O in Juan de Fuca Ridge basaltic glasses. Earth and Planetary Science Letters 90, 87–104.

Dixon, J.E., Stolper, E.M., Holloway, J.R., 1995a. An experimental study of water and carbon dioxide solubilities in mid-ocean ridge basaltic liquids. Part I: calibration and solubility models. Journal of Petrology 36, 1607–1631.

Dixon, J.E., Stolper, E.M., Holloway, J.R., 1995b. An experimental study of water and carbon dioxide solubilities in mid-ocean ridge basaltic liquids. Part II: applications to degassing. Journal of Petrology 36, 1633–1646.

Dunn, R.A., Toomey, D.R., Detrick, R.S., Wilcock, W.S.D., 2001. Continuous mantle melt supply beneath an overlapping spreading center on the East Pacific Rise. Science 291, 1955–1958.

Eiler, J.M., 2001. Oxygen isotope variations of basaltic lavas and upper mantle rocks. Reviews in Mineralogy and Geochemistry 43, 319–364.

Eiler, J.M., Farley, K.A., Valley, J., Hofmann, A.W., Stolper, E.M., 1996. Oxygen isotope constraints on the sources of Hawaiian volcanism. Earth and Planetary Science Letters 144, 453–468.

Fornari, D.J., 2003. A new deep-sea towed digital camera and multi-rock coring system. EOS, Transactions American Geophysical Union 84, 69–76.

Garcia, M.O., Muenow, D.W., Aggrey, K.E., O'Neil, J.R., 1998. Major element, volatile and stable isotope geochemistry of Hawaiian submarine tholeiitic glasses. Journal of Geophysical Research 94, 10,525–10,538.

Gautason, B., Muehlenbach, K., 1998. Oxygen isotopic fluxes associated with high-temperature processes in the rift zones of Iceland. Chemical Geology 145, 275–286.

Ghiorso, M.S., Sack, R.O., 1995. Chemical mass transfer in magmatic processes. IV. A revised and internally consistent thermodynamic model for the interpolation and

extrapolation of liquid–solid equilibria in magmatic systems at elevated temperatures and pressures. Contributions to Mineralogy and Petrology 119, 197–212.
Gillis, K.M., 2008. The roof of an axial magma chamber: a hornfelsic heat exchanger. Geology 36, 299–302.
Gillis, K.M., Coogan, L.A., 2002. Anatectic migmatites from the roof of an ocean ridge magma chamber. Journal of Petrology 43, 2075–2095.
Gillis, K.M., Muehlenbach, K., Stewart, M., Gleeson, T., Karson, J.A., 2001. Fluid flow patterns in fast spreading East Pacific Rise crust exposed at Hess Deep. Journal of Geophysical Research 106, 26,311–26,329.
Godard, M., Awaji, S., Hansen, H., Hellebrand, E., Brunelli, D., Johnson, K.T.M., Yamasaki, T., Maeda, J., Abratis, M., Christie, D.M., Kato, Y., Mariet, C., Rosner, M., 2009. Geochemistry of a long in-situ section of intrusive slow-spread oceanic lithosphere: results from IODP Site U1309 (Atlantis Massif, 30°N Mid-Atlantic Ridge). Earth and Planetary Science Letters 279, 110–122.
Goss, A., Perfit, M., Ridley, W.I., Rubin, K.H., Kamenov, G., Soule, A.S., Fundis, A., Fornari, D.J., 2010. Geochemistry of lavas from the 2005–2006 eruption at the East Pacific Rise, 9°46′N–9°56′N: implications for ridge crest plumbing and decadal changes in magma chamber compositions. Geochemistry, Geophysics, Geosystems 11, 1–35.
Grimes, C.B., Ushikubo, T., Valley, J.W., 2010. Low δ18O (Zrc) in plagiogranites at Oman: evidence for remelting. Geochemica et Cosmochimica Acta 74, A355.
Grimes, C.B., Ushikubo, T., John, B.E., Valley, J., 2011. Uniformly mantle-like $\delta^{18}O$ in zircons from oceanic plagioranites and gabbros. Contributions to Mineralogy and Petrology 161, 13–33.
Harding, A.J., Kent, A.J.R., Orcutt, J.A., 1993. A multichannel seismic investigation of upper crustal structure at 9°N on the East Pacific Rise: implications for crustal accretion. Journal of Geophysical Research 98, 13,925–13,944.
Johnson, E.R., Wallace, P., Delgado Granados, H., Manea, V.C., Kent, A.J.R., Bindeman, I.N., Donegan, C.S., 2009. Subduction-related volatile recycling and magma generation beneath Central Mexico: insights from melt inclusions, oxygen isotopes and geodynamic models. Journal of Petrology 50, 1729–1764.
Kelley, D.S., Delaney, J.R., 1987. Two-phase separation and fracturing in mid-ocean ridge gabbros at temperatures greater than 700 °C. Earth and Planetary Science Letters 83, 53–66.
Kent, A.J.R., Harding, A.J., Orcutt, J.A., 1993. Distribution of magma beneath the East Pacific Rise near 9°03′N overlapping spreading center from forward modeling of CDP data. Journal of Geophysical Research 98, 13,971–13,995.
Kent, A.J.R., Norman, M.D., Hutcheon, I.D., Stolper, E.M., 1999. Assimilation of seawater-derived components in an oceanic volcano: evidence from matrix glasses and glass inclusions from Loihi seamount, Hawaii. Chemical Geology 156, 299–319.
Kent, G.M., Singh, S.C., Harding, A.J., Sinha, M.C., Orcutt, J.A., Barton, P.J., White, R.S., Bazin, S., Hobbs, R.W., Tong, C.H., Pye, J.W., 2000. Evidence from three-dimensional seismic reflectivity images for enhanced melt supply beneath mid-ocean ridge discontinuities. Nature 406, 614–618.
Kent, A.J.R., Peate, D.W., Newman, S., Stolper, E.M., Pearce, J.A., 2002. Chlorine in submarine glasses from the Lau Basin: seawater contamination and constraints on the composition of slab-derived fluids. Earth and Planetary Science Letters 202, 361–377.
Koepke, J., Feig, S.T., Snow, J., Freise, M., 2004. Petrogenesis of oceanic plagiogranites by partial melting of gabbros: an experimental study. Contributions to Mineralogy and Petrology 146, 414–432.
Koepke, J., Berndt, J., Feig, S.T., Holtz, F., 2007. The formation of SiO_2-rich melts within the deep oceanic crust by hydrous partial melting of gabbros. Contributions to Mineralogy and Petrology 153, 67–84.
Langmuir, C.H., Bender, J.F., Batiza, R., 1986. Petrological and tectonic segmentation of the East Pacific Rise, 5°30′–14°30′N. Nature 322, 422–429.
le Roux, P.J., Shirey, S.B., Hauri, E.H., Perfit, M.R., Bender, J.F., 2006. The effects of variable sources, processes and contaminants on the composition of northern EPR MORB (8–10 N and 12–14 N): evidence from volatiles (H_20, CO_2, S) and halogens (F, Cl). Earth and Planetary Science Letters 251, 209–231.
Macdonald, K.C., Fox, P.J., 1983. Overlapping spreading centers: new accretion geometry on the East Pacific Rise. Nature 302, 55–58.
Mandeville, C.W., Webster, J.D., Rutherford, M.J., Taylor, B.E., Timbal, A., Faure, K., 2002. Determination of molar absorptivities for infrared absorption bands of H2O in andesitic glass. American Mineralogist 87, 813–821.
Mathez, E.A., 1976. Sulfur solubility and magmatic sulfides in submarine basalt glass. Journal of Geophysical Research 81.
Matsuhisa, Y., Matsubaya, O., Sakai, H., 1973. Oxygen isotope variations in magmatic differentiation processes of the volcanic rocks in Japan. Contributions to Mineralogy and Petrology 39, 277–288.
Michael, P., Cornell, W.C., 1998. Influence of spreading rate and magma supply on crystallization and assimilation beneath mid-ocean ridges: evidence from chlorine and major element chemistry of mid-ocean ridge basalts. Journal of Geophysical Research 103, 18,325–18,356.
Michael, P., Schilling, J.G., 1989. Chlorine in mid-ocean ridge magmas: evidence for assimilation of seawater-influenced components. Geochimica Cosmochemica Acta 53, 3131–3143.
Muehlenbach, K., Byerly, G.R., 1982. ^{18}O-Enrichment of silicic magmas caused by crystal fractionation at the Galapagos Spreading Center. Contributions to Mineralogy and Petrology 79, 76–79.
Muehlenbach, K., Clayton, R.N., 1972. Oxygen isotope studies of fresh and weathered submarine basalts. Canadian Journal of Earth Science 2, 172–184.
Newman, S., Lowenstern, J.B., 2002. VOLATILECALC: a silicate melt–H_2O–CO_2 solution model written in Visual Basic for excel. Computers and Geosciences 28, 597–604.
Niu, Y., Gilmore, T., Mackie, S., Greig, A., Bach, W., 2002. Mineral chemistry, whole-rock compositions, and petrogenesis of Leg 176 gabbros: data and discussion. College Station, Ocean Drilling Program.
O'Hara, M.J., 1977. Geochemical evolution during fractional crystallization of a periodically refilled magma chamber. Nature 266, 503–507.
Pedersen, R.B., Malpas, J., 1984. The origin of oceanic plagiogranites from the Karmoy ophiolite, western Norway. Contributions to Mineralogy and Petrology 88, 36–52.
Perfit, M.R., Fornari, D.J., Malahoff, A., Embley, R.W., 1983. Geochemical studies of abyssal lavas recovered by DSRV Alvin from Eastern Galapagos Rift, Inca Transform, and Ecuador Rift 3. Trace element abundances and petrogenesis. Journal of Geophysical Research 88, 10,551–10,572.
Perfit, M.R., Fornari, D.J., Smith, M.C., Bender, J.F., Langmuir, C.H., Hayman, N.W., 1994. Small-scale spatial and temporal variations in mid-ocean ridge crest magmatic processes. Geology 22, 375–379.
Perfit, M.R., Ridley, W.I., Jonasson, I.R., 1999. Geologic, petrologic and geochemical relationships between magmatism and massive sulfide mineralization along the eastern Galapagos Spreading Center. Reviews in Economic Geology 8, 75–99.
Reynolds, J.R., 1995. Segment-scale systematic of mid-ocean ridge magmatism and geochemistry. Palisades: Columbia University, 483.
Sempere, J.-C., Macdonald, K.C., 1986. Deep-tow studies of the overlapping spreading centers at 903′ N on the East Pacific Rise. Tectonics 5, 881–900.
Sigurdsson, H., 1977. Generation of Icelandic rhyolites by melting of plagiogranites in the oceanic layer. Nature 269, 25–28.
Smith, M.C., Perfit, M.R., Fornari, D.J., Ridley, W.I., Edwards, M.H., Kurras, G.J., Von Damm, K.L., 2001. Magmatic processes and segmentation at a fast spreading mid-ocean ridge: detailed investigation of an axial discontinuity on the East Pacific Rise crest at 9°37′N. Geochemistry, Geophysics, Geosystems 2, 1–32.
Sparks, J.W., 1995. Geochemistry of the Lower Sheeted Dike Complex, Hole 504B, Leg 140. Proceedings of the Ocean Drilling Program. Scientific Results 137 (140), 81–97.
Spicuzza, M.J., Valley, J.W., Kohn, M.J., Girard, J.P., Fouillac, A.M., 1998. The rapid heating, defocused beam technique: a CO_2-laser-based method for highly precise and accurate determination of $\delta^{18}O$ values of quartz. Chemical Geology 144, 195–203.
Stewart, M.A., Klein, E.M., Karson, J.A., 2002. Geochemistry of dikes and lavas from the north wall of the Hess Deep Rift: insights into the four-dimensional character of crustal construction at fast spreading mid-ocean ridges. Journal of Geophysical Research 107, 2238.
Sun, W.D., Binns, R.A., Fan, A.C., Kamenetsky, V.S., Wysoczanski, R., Wei, G.J., Hu, Y.H., Arculus, R.J., 2007. Chlorine in submarine volcanic glasses from the eastern Manus basin. Geochemica et Cosmochimica Acta 71, 1542–1552.
Taylor, H.P.J., 1968. The oxygen isotope geochemistry of igneous rocks. Contributions to Mineralogy and Petrology 19, 1–71.
Tong, C.H., Pye, J.W., Barton, P.J., White, R.S., Sinha, M.C., Singh, S.C., Hobbs, R.W., Bazin, S., Harding, A.J., Kent, G.M., Orcutt, J.A., 2002. Asymmetric melt sills and upper crustal construction beneath overlapping ridge segments: implications for the development of melt sills and ridge crests. Geology 30, 83–86.
Unni, C.K., Schilling, J.G., 1978. Cl and Br degassing by volcanism along the Reykjanes Ridge and Iceland. Nature 272, 19–23.
Valley, J., Kitchen, N., Kohn, M.J., Niendorf, C.R., Spicuzza, M.J., 1995. UWG-2, a garnet standard for oxygen isotope ratios: strategies for high precision and accuracy with laser heating. Geochemica et Cosmochimica Acta 59, 5223–5231.
Von Damm, K.L., Buttermore, L.G., Oosting, S.E., Bray, A.M., Fornari, D.J., Lilley, M., Shanks, W.C., 1997. Direct observation of the evolution of a seafloor 'black smoker' from vapor to brine. Earth and Planetary Science Letters 149, 101–111.
Wallace, P., Carmichael, I.S.E., 1992. Sulfur in basaltic magmas. Geochemica et Cosmochimica Acta 56, 1863–1874.
Wanless, V.D., Perfit, M.R., Ridley, W.I., Klein, E.M., 2010. Dacite petrogenesis on mid-ocean ridges: evidence for oceanic crustal melting and assimilation. Journal of Petrology 51, 2377–2410.
Webster, J.D., Kinzler, R.J., Mathez, E.A., 1999. Chloride and water solubility in basalts and andesite melts and implications for magmatic degassing. Geochemica et Cosmochimica Acta 63, 729–738.
White, S.M., Mason, J.L., Macdonald, K.C., Perfit, M.R., Wanless, V.D., Klein, E.M., 2009. Significance of widespread low effusion rate eruptions over the past two million years for delivery of magma to the overlapping spreading centers at 9°N East Pacific Rise. Earth and Planetary Science Letters 280, 175–184.

Please cite this article as: Wanless, V.D., et al., Volatile abundances and oxygen isotopes in basaltic to dacitic lavas on mid-ocean ridges: The role of assimilation at spreading centers, Chem. Geol. (2011), doi:10.1016/j.chemgeo.2011.05.017